SPEKTRA: Jurnal Fisika dan Aplikasinya
Volume 9, Issue 3, December 2024
Homepage: doi.org/10.21009/SPEKTRA

DOI: doi.org/10.21009/SPEKTRA.093.04

Geochemical and Magnetic Suseptibility Analysis for Critical Minerals Detection in Igneous Rocks and Beach Sand

Yensi Hariyanto[1], Siti Zulaikah[1,*], Cahyo Aji Hapsoro[1], Shofi Maulida[1], Hanif 'Izzudin Zakly[1], Nordiana Mohd Muztaza[2], Daeng Achmad Suaidi[1], Aditya Pratama[3], Hamdi[4]

[1]*Department of Physics, Faculty Mathematics and Natural Sciences, Universitas Negeri Malang, Jl. Semarang 5, Malang, 65145, Indonesia*
[2]*School of Physics,Universiti Sains Malaysia, Penang Island, 11800, Malaysia*
[3]*Research Center for Geological Disaster, National Research and Innovation Agency (BRIN), Bandung 40135, Indonesia*
[4]*Departemen of Physics, Faculty Mathematics and Natural Sciences, Universitas Negeri Padang, West Sumatra, 25171, Indonesia*

*Corresponding Author Email: siti.zulaikah.fmipa@um.ac.id

Received: 22 October 2024
Revised: 11 December 2024
Accepted: 13 December 2024
Online: 16 December 2024
Published: 30 December 2024

SPEKTRA: Jurnal Fisika dan Aplikasinya
p-ISSN: 2541-3384
e-ISSN: 2541-3392

ABSTRACT

Critical minerals are an important natural resource that will continue to be necessary for modern industries. This study aims to determine the distribution of critical minerals based on geochemical data and magnetic susceptibility. Samples were taken from Lenggoksono beach, Southern Malang. The determination of chemical elements was conducted using X-ray fluorescence (XRF). Rare Earth Elements (REE) were identified using Inductively Coupled Plasma–Optical Emission Spectrometry (ICP-OES). Magnetic susceptibility measurements were carried out using a Barrington Magnetic Susceptibility Meter (MS2B). The results showed that the dominant elements were Silica Oxide, SiO_2 (70 Wt%), Iron Oxide, Fe_2O_3 (14.05 Wt%), and Calcium Oxide CaO (5.57 Wt%), which were categorized as critical minerals. The average REE elements detected were Cerium, Ce (6.75 mg/kg), Gadolinium, Gd (5.98 mg/kg), Neodymium, Nd (13.56 mg/kg), Praseodymium, Pr (6.62 mg/kg), Terbium, Tb (5.57 mg/kg), and Yttrium, Y (10.98 mg/kg). The magnetic susceptibility ranges from 13.27 to 4143.47 × $10^{-8}m^3$/kg. Pearson's Correlation analysis revealed a significant correlation between low-frequency magnetic susceptibility (χ_{lf}) and high-frequency magnetic susceptibility (χ_{hf}) with a significance level of 0.01. χ_{lf} and χ_{hf} also

showed a significant correlation with Gd, with a correlation value of $R^2 = 0.84$ and a significance level of 0.05. These results indicate that the presence of one critical mineral can serve as a clue to the presence of other critical minerals, and magnetic susceptibility can be used as a proxy indicator for critical minerals in natural materials.

Keywords: critical minerals, Lenggoksono, REE, magnetic susceptibility

INTRODUCTION

Modern industries continue to experience an increasing need for critical minerals in line with technological developments and climate change mitigation efforts [1-2]. The production of critical minerals is currently dominated by one country, namely China, which has 85% of the global processing capacity for Rare Earth Elements (REE) [3]. With the increasing demand for REEs, Indonesia needs to develop a sustainable resource management strategy.

As one of the countries with abundant geological resource potential, Indonesia has an excellent opportunity to contribute to meeting the global need for critical minerals. Metallic minerals such as gold, silver, copper, nickel, tin, zinc, iron, aluminum, and rare earth metals, as well as non-metallic rocks such as limestone, kaolin, zircon, phosphate, gypsum, and potassium-containing rocks, are some of the types of minerals found in Indonesia [4-5]. The presence of critical mineral sources can be found in igneous rocks.

Igneous rocks formed from magical activity in Lenggoksono are prime targets in the search for critical minerals. Minerals such as rare earth elements (REEs), lithium, and cobalt have an important role in various high-tech applications, including renewable energy and electronics [6-7]. However, identifying and quantifying these critical minerals is often challenging due to their uneven distribution and relatively low concentration in the host rock. When a mineral is considered important to the country's economy and security and is vulnerable to global supply risks, especially when REE production comes from limited mineral resources, it is classified as a critical mineral.

Geochemical analysis and magnetic susceptibility produce important data for detecting minerals and critical characterization in rock formations. This method involves collecting and interpreting chemical data from coastal rocks and sand samples, which can reveal patterns and anomalies associated with mineralization. With advances in analytics and data processing techniques. Modern geochemical analysis allows for the detection of critical minerals with a higher level of sensitivity and accuracy, even at very low concentrations [8-9].

This study aims to analyze the critical distribution of minerals in the Lenggoksono region. This analysis is based on igneous rock and sand samples obtained in the Lenggoksono area.

METHOD

Geographical Location and Geological Conditions of Lenggoksono

Purwodadi Village has an area of 1041 Ha, divided into three hamlets: Balaearjo, Purwodadi, and Lenggoksono. Geographically, this region is located at 8°20’0’’LS-82o5’0 “S and 112°47’0’’BT-112o52’0’’E [10]. Based on the geological map shown in FIGURE 1, the Lenggoksono area with mandalika formations is dominated by andesite, basalt, tract, dacite and dispersed andesite breccia (Tomm) lava. Members of the Mandalika Formation Tuff which is dominated by rhyolite-dacite tuft, pumice tuff breccia (Tomi). Swamp and river deposits are dominated by gravel, sand, clay and plant residues (Qas) [11].

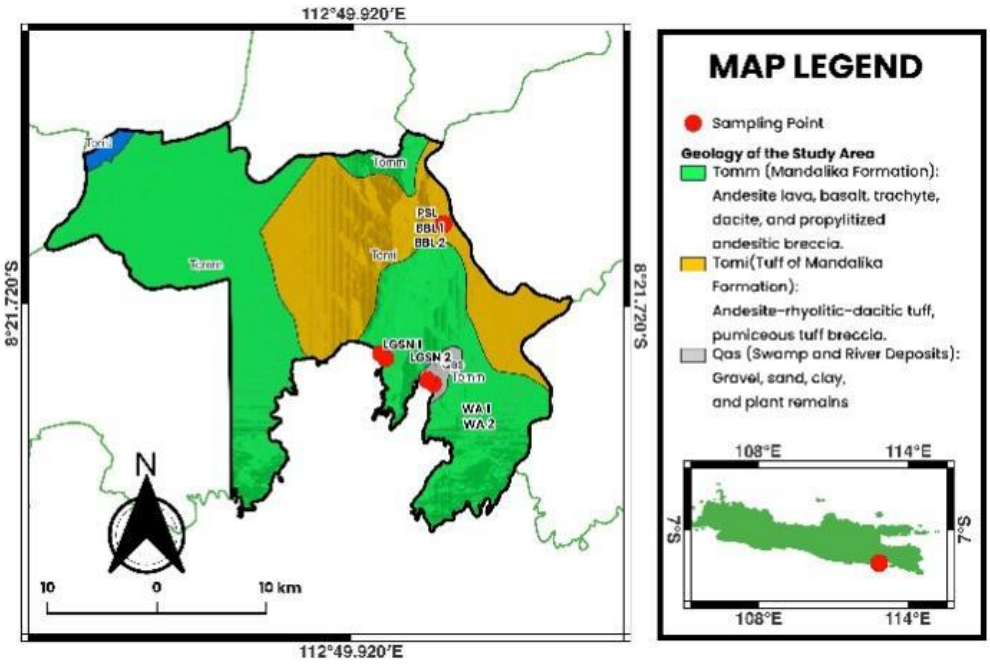

FIGURE 1. Geological map of Lenggoksono (Created by QGIS)

Sampling and Sample Preparation

This research was carried out in several stages, starting with a literature study on Rare Earth Elements (REE) and critical minerals. Furthermore, the identification of sampling locations in the Lenggoksono area was carried out. The sampling points are shown in detail in FIGURE 2. The sampling process can be seen in FIGURE 3(a); the samples taken are in the form of igneous rocks found in the Lenggoksono River and sand from the Lenggoksono River, Wedi Awu Beach, and Lenggoksono Rivers.

The next stage is the sample process carried out in the laboratory. Sample preparation begins with scraping the sample using mortar, as seen in FIGURE 3(b), followed by drying on a plastic plate lined with perforated plastic wrap. Next, we weigh the samples and perform X-ray fluorescence (XRF) tests to identify chemical elements associated with critical minerals [12].

Measurement

In general, XRF is used to determine the constituent elements of a material. XRF analysis can be done qualitatively and quantitatively [13-14]. In addition to the XRF test, this study also uses the ICP-OES technique to analyze the content of Rare Earth Element (REE) and the magnetic susceptibility test as shown in FIGURE 3(c) is a sample that is ready for magnetic susceptibility test. Magnetic susceptibility is measured with the MS2B magnetic susceptibility meter. Magnetic susceptibility can be used to determine the indication of magnetic mineral content in nature in the presence of Fe. The magnetic susceptibility value can be used to determine the properties of magnetic minerals [15].

Meanwhile, measurements with ICP-OES begin by inserting a sample in liquid form into a nebulizer. These aerosols are then delivered to the main plasma, where the ionization of atoms and the excitation of electrons occur. When an electron returns to its base energy level, the energy is released in the form of radiation of a specific wavelength. This radiation is then detected by sensors to identify and measure the concentration of the elements in the sample [16-18]. The data then analyzed with statistical software (SPSS). This test was carried out to determine the linear relationship between one variable and another variable between critical mineral elements and REE elements, as well as magnetic susceptibility that can indicate mineral dispersion [19].

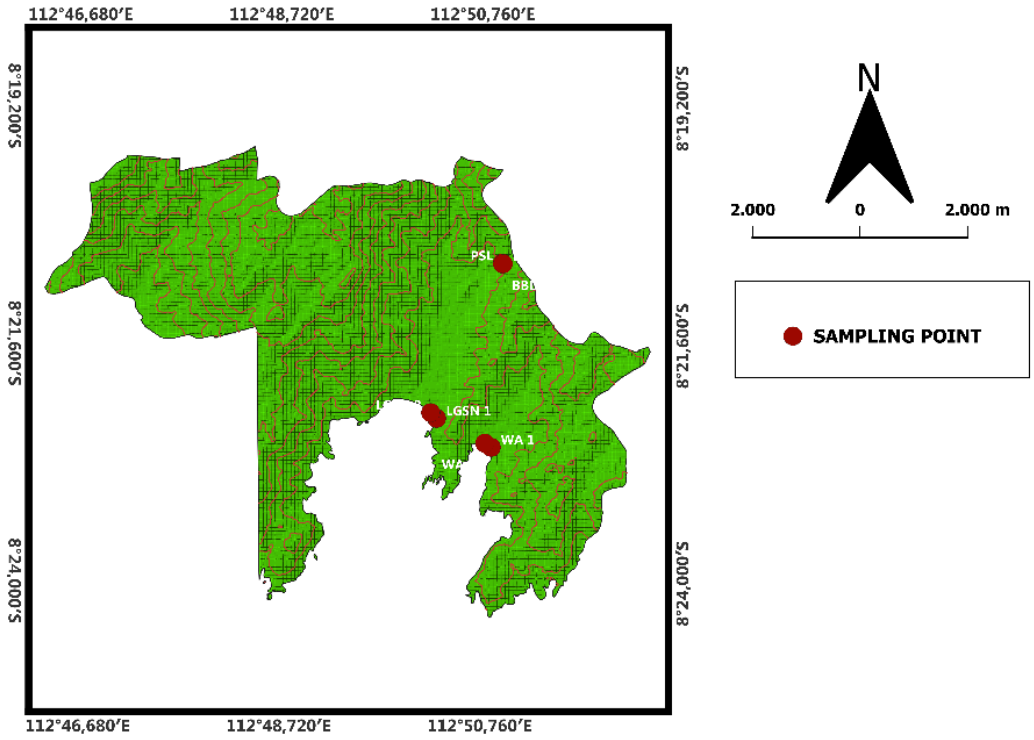

FIGURE 2. Sampling Location Point (Created by QGIS)

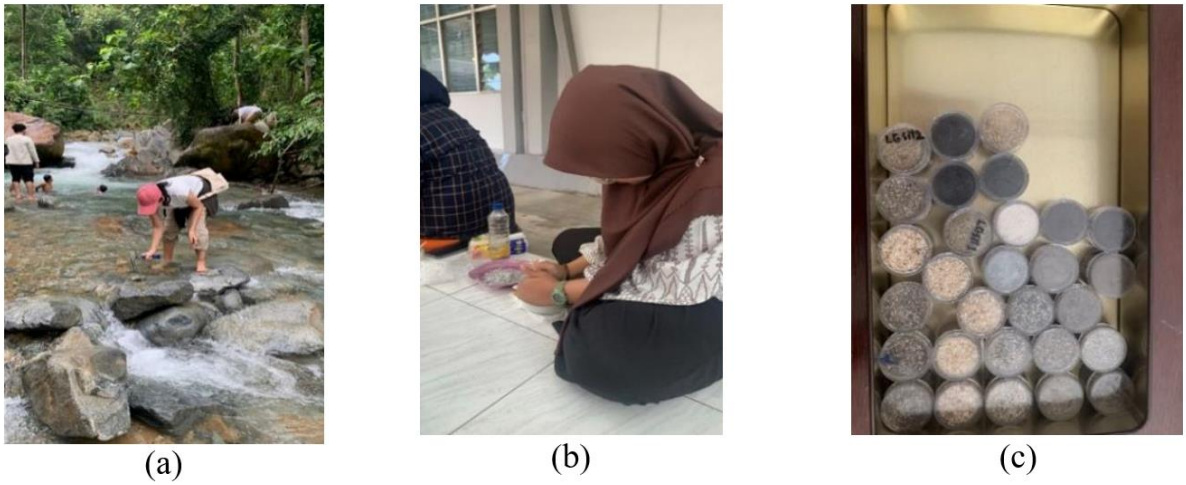

FIGURE 3. (a) Sampling, (b) Scraping of samples, (c) Samples ready for testing

RESULTS AND DISCUSSION

Geochemistry of Igneous Rocks

The chemical element content test results of the selected sample can be seen in TABLE 1. The composition of chemical elements showed that SiO_2 content was the dominant element in all samples, ranging from 55.1% by weight to 81.88% by weight Fe_2O_3 compounds had varying values, with the highest content of 23.1% by weight (PSL) and the lowest at 6.76% by weight (BBL 2). Al_2O_3 compounds were detected in PSL, BBL 1 and BBL 2 samples with concentrations of 12% by weight to 13% by weight CaO compounds varied from 2.6% by weight to 13% by weight with BBL 1 having the highest concentration. The full content of the compound can be seen in TABLE 1.

Rare Earth Elements (REE)

The total REE concentration ranged from 27.36 mg/kg (BBL 2) to 79.35 mg/kg (BBL 1) shown in TABLE 2. The BBL 1 sample showed the most significant REE dominance with total REE concentrations nearly tripling compared to the lowest sample, indicating mineralization potential zones of interest for further exploration [20-21]. The distribution of Light Rare Earth Elements (LREE) and Heavy Rare Earth Elements (HREE) varied between samples. LREE (Ce, Nd, Pr) is generally more dominant in most samples, except in WA 1 and BBL 2 where HREE (Gd, Tb, Y) is more prominent. The high LREE content is related to the type of host rock such as granite or granitoid rocks that are rich in LREE-carrying minerals. The dominance of LREE, especially in LGSN 1, LGSN 2, and PSL samples, is consistent with patterns commonly found in many terrestrial REE deposits [22]. However, the relatively high enrichment of HREE in some samples, especially BBL 1 and WA 1, is interesting from an economic perspective because HREE is generally rarer and of higher value [23]. The magnetic REE distribution map is shown in FIGURE 4. FIGURE 4 (a) shows the distribution of Cerium (Ce) in the Lenggoksono region, based on the map this element has the highest concentration at the LGSN 1 point with an average of 7.52 mg/kg. In the Yttrium (Y) element, the distribution map is shown in FIGURE 4 (b) where the location point with the highest average is BBL 1 of 12.94 mg/kg, indicating that at LGSN 1 and BBL 1 are potential REE zones.

TABLE 1. Composition of Enggoksono samples measured by X-Ray Fluorescene

Compound	**Sample Name**						
Oxides (wt%)	**LGSN 1**	**LGSN 2**	**WA 1**	**WA 2**	**PSL**	**BBL 1**	**BBL 2**
Al_2O_3	0.00	0.00	0.00	0.00	13.00	12.00	13.00
SiO_2	77.40	81.80	76.00	74.70	55.90	55.10	73.50
SO_3	0.00	0.00	0.00	0.00	0.00	1.90	2.20
P_2O_5	0.00	0.00	0.00	0.00	0.95	0.00	0.00
K_2O	1.10	0.84	0.95	0.90	1.61	0.48	0.54
CaO	2.98	3.62	7.12	6.98	2.60	13.00	2.72
TiO_2	1.31	1.40	2.32	2.11	1.26	1.15	0.79
V_2O_5	0.04	0.03	0.07	0.08	0.06	0.07	0.02
Cr_2O_3	0.04	0.04	0.05	0.05	0.06	0.05	0.03
MnO	0.28	0.24	0.20	0.21	0.49	0.16	0.17
Fe_2O_3	13.70	11.6	12.90	14.60	23.10	15.70	6.76
CuO	0.07	0.06	0.06	0.07	0.09	0.05	0.04
ZnO	0.05	0.03	0.03	0.00	0.13	0.00	0.02
MoO_3	2.70	0.00	0.00	0.00	0.00	0.00	0.00
Eu_2O_3	0.20	0.22	0.20	0.20	0.32	0.20	0.10
Yb_2O_3	0.00	0.00	0.00	0.00	0.00	0.00	0.03
Re_2O_7	0.10	0.10	0.10	0.00	0.10	0.00	0.07

TABLE 2. Lenggoksono Rare Earth Element Data

Nama	Rare Earth Element (ppm)						LREE	HREE	Total	**Tmag**	**Tnon**
Sampel	Ce	Gd	Nd	Pr	Tb	Y			REE		**Mag**
LGSN 1	11.72	4.15	14.88	10.87	<0.01	9.11	37.47	13.27	50.74	41.63	9.11
LGSN 2	6.74	5.06	18	7.47	<0.01	8.44	32.21	13.51	45.72	37.28	8.44
WA 1	5.61	8.87	9.01	4.86	8.44	9.91	19.48	27.22	46.7	36.79	9.91
WA 2	4.41	6.78	10.81	4.4	8.44	9.75	19.62	24.97	44.59	34.84	9.75
PSL	6.88	5.22	13.3	7.81	9.37	9.42	27.99	24.01	52.00	42.58	9.42
BBL 1	8.07	7.66	23.36	10.95	12.76	16.55	42.38	36.97	79.35	62.80	16.55
BBL 2	3.84	4.16	5.62	<0.01	<0.01	13.72	9.47	17.89	27.36	13.64	13.72
Average	6.75	5.98	13.57	7.72	9.75	10.99	26.95	22.55	49.50	38.51	11.00

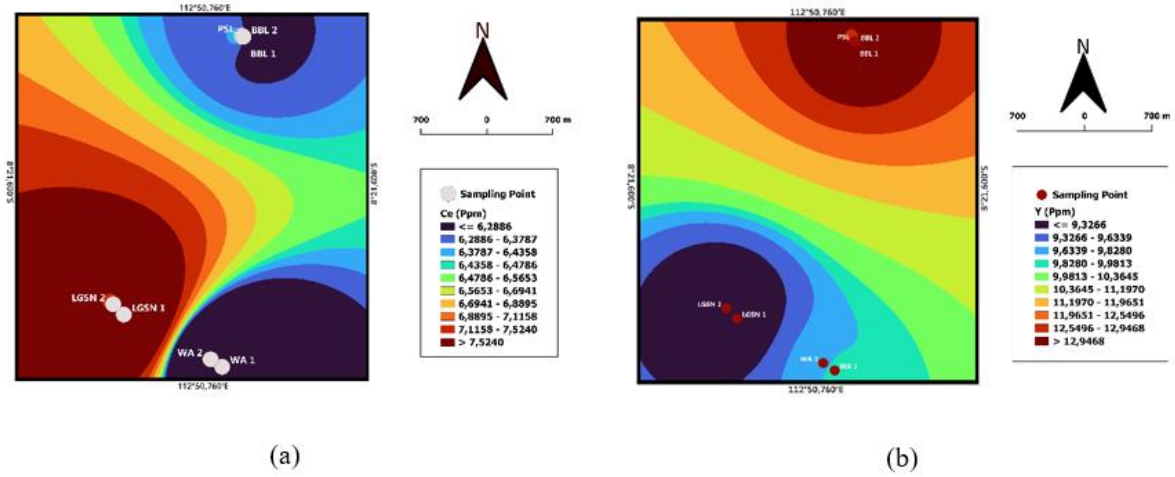

(a) (b)

FIGURE 4. Map of the distribution of REE in the Lenggoksono area (a) element Ce, (b) element Y.

Magnetic Susceptibility

Analysis of magnetic susceptibility tests on 7 samples showed significant variation in the material's magnetic properties. The value of low-frequency magnetic susceptibility (χ_{lf}) ranges from 13.27 × 10^{-8} m3/kg (BBL 2) up to 4143.47 × 10^{-8} m3/kg (WA 1), indicating a wide range of magnetic mineral content [24]. The WA 1 sample showed the highest susceptibility, indicating significant concentrations of ferromagnetic minerals. High-frequency vulnerability (χ_{hf}) shows a similar pattern to χ_{lf}, with the lowest value at BBL 2 (12 × 10^{-8} m3/kg) and the highest in WA 1 (4137 × 10^{-8} m3/kg). The difference between χ_{lf} and χ_{hf} provides information about the presence of very fine superparamagnetic particles, which are generally related to soil formation or weathering processes. Frequency-dependent vulnerability (χ_{fd}%) varied from 0.01% (WA 3) to 8.27% (BBL 2). The high χ_{fd}% value of BBL 2 indicates a significant proportion of very fine-sized superparamagnetic particles (<0.03 μm), which are often associated with in situ soil formation or intensive weathering processes [25].

TABLE 3. Magnetic susceptibility data

No	Sample Name	χ_{lf} ($10^{-8}m^3/kg$)	χ_{hf} ($10^{-8}m^3/kg$)	χ_{fd} (%)
1	LGSN 1	346.67	345.00	0.35
2	LGSN 2	661.03	659.40	0.29
3	WA 1	4143.47	4137.00	0.13
4	WA 2	1015.37	1013.40	0.16
5	PSL	161.13	160.30	0.62
6	BBL 1	1936.23	1935.50	0.05
7	BBL 2	13.27	12.00	8.27
Average		1182.45	1180.37	1.41

Pearson's Correlation

The next part of the study analyzes *Pearson Correlation* between the susceptivity test data, XRF and the OES ICP data. The goal was to find a relationship between two strong or significant variables marked with (*) for a significance of 0.05 and (**) for a significance of

0.01 [26-27]. Using SPSS software, there is an inverse relationship between several pairs indicating that there is a tendency for one variable to act in the opposite direction to another, Al_2O_3 and SiO_2; SO_3 and CuO; Yb_2O_3 and REEmag; χ_{fd} and REEmag with a significance value of 0.05, if the concentration of Al_2O_3 increases, the concentration of SiO_2 tends to decrease. There are also several pairs with a directly proportional or positive relationship showing the relationship between the magnetic properties of an area and the potential presence of minerals containing rare earth elements, namely the elements χ_{lf} and χ_{hf}, Gd; χ_{hf} and Gd; χ_{fd} and Yb_2O_3; Nd and LREE, REEmag; Pr and LREE, REEmag; Tb and HREE; Y and SO_3, REEnonmag; SO_3 and REEnonmag; P_2O_5 and MnO, ZnO; K_2O and MnO, CuO, ZnO; Cr_2O_3 and Fe_2O_3, Eu_2O_3; MnO and CuO, ZnO; Fe_2O_3 and Eu_2O_3; LREE dan REEmag; TotalREE and REEmag with a significance of 0.01. The correlation between the element REE and the magnetic susceptibility value of Gadolinium (Gd) and xlf where the correlation between the two is directly proportional. The graph between the correlation between the two is illustrated in FIGURE 5(a) with $R^2 = 0.84$, showing that about 84.09% of the variation in one variable can be explained by the variation in the other variable, indicating a very strong relationship and in FIGURE 5(b) with $R^2 = 0.59$. However, this value is lower compared to FIGURE 5(a), it still shows a significant relationship between the two variables.

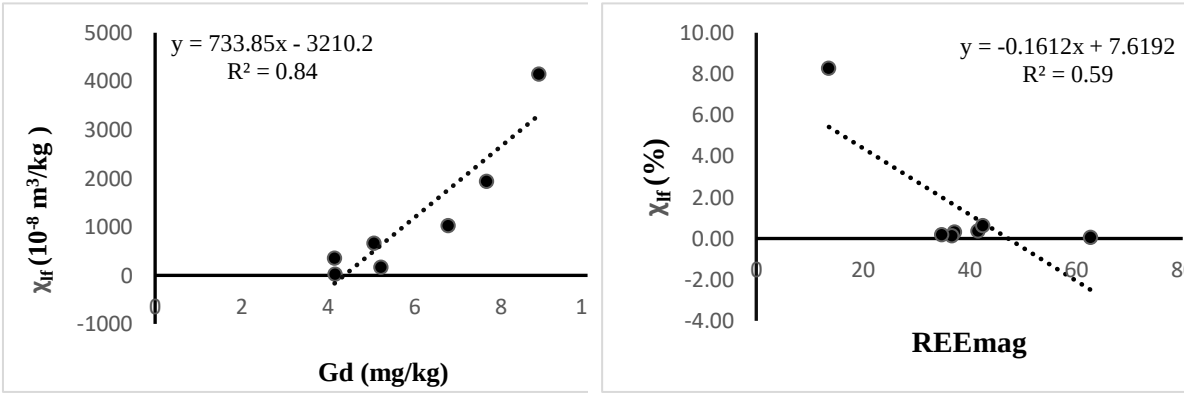

(a) (b)

FIGURE 5. Correlation graph between (a) χ_{lf}-Gd (b) χ_{lf}-SiO_2

TABLE 4. Pearson Correlation

	Xlf	Xhf	Xfd	Ce	Gd	Nd	Pr	Tb	Y	Al_2O_3	SiO_2
Xlf	1										
Xhf	**1.000****	1									
Xfd	-0.391	-0.391	1								
Ce	-0.124	-0.124	-0.474	1							
Gd	**0.917****	**0.917****	-0.480	-0.237	1						
Nd	0.010	0.010	-0.603	0.580	0.144	1					
Pr	0.028	0.028	-0.744	**0.869***	0.070	**0.858***	1				
Tb	0.499	0.500	-0.469	-0.133	**0.765***	0.317	0.259	1			
Y	0.096	0.097	0.372	-0.127	0.222	0.262	-0.019	0.380	1		
Al_2O_3	-0.328	-0.327	0.508	-0.190	-0.184	0.044	-0.118	0.287	0.674	1	
SiO_2	0.040	0.039	0.107	-0.076	-0.206	-0.393	-0.338	-0.741	-0.562	**-0.785***	1
SO_3	-0.130	-0.130	0.685	-0.246	-0.076	0.031	-0.270	0.043	**0.921****	0.714	-0.361
P_2O_5	-0.309	-0.309	-0.115	0.021	-0.185	-0.020	0.135	0.309	-0.231	0.493	-0.609
K_2O	-0.184	-0.185	-0.389	0.255	-0.184	-0.125	0.240	0.085	-0.696	-0.074	-0.166
CaO	0.586	0.586	-0.377	-0.003	**0.770***	0.543	0.326	0.742	0.653	0.086	-0.431
TiO_2	0.705	0.705	-0.576	-0.202	0.705	-0.200	-0.064	0.354	-0.466	-0.709	0.329
V_2O_5	0.495	0.495	-0.627	-0.133	0.737	0.109	0.183	**0.840***	-0.028	-0.177	-0.356
Cr_2O_3	0.235	0.235	-0.723	0.150	0.420	0.359	0.485	0.717	-0.243	0.072	-0.582
MnO	-0.384	-0.384	-0.253	0.248	-0.331	0.006	0.272	0.092	-0.503	0.217	-0.373
Fe_2O_3	-0.033	-0.032	-0.620	0.294	0.170	0.368	0.551	0.630	-0.198	0.213	-0.678
CuO	-0.252	-0.252	-0.471	0.223	-0.175	-0.041	0.274	0.140	-0.704	-0.122	-0.173
ZnO	-0.320	-0.320	-0.112	0.244	-0.347	-0.084	0.199	0.015	-0.439	0.297	-0.358
MoO_3	-0.253	-0.253	-0.154	**0.831***	-0.444	0.098	0.482	-0.454	-0.277	-0.353	0.280
Eu_2O_3	-0.029	-0.029	-0.690	0.303	0.103	0.376	0.550	0.434	-0.446	0.016	-0.447
Yb_2O_3	-0.354	-0.354	**0.998****	-0.487	-0.442	-0.594	-0.750	-0.454	0.404	0.493	0.119
Re_2O_7	-0.057	-0.058	0.064	0.255	-0.373	-0.278	-0.011	-0.548	-0.609	-0.178	0.351
LREE	-0.014	-0.014	-0.670	**0.821***	0.043	**0.937****	**0.978****	0.220	0.099	-0.061	-0.333
HREE	0.552	0.552	-0.272	-0.182	**0.784***	0.327	0.174	**0.940****	0.645	0.383	-0.718
TotalREE	0.291	0.291	-0.646	0.511	0.460	**0.874***	**0.822***	0.676	0.426	0.164	-0.639
REEmag	0.291	0.292	**-0.769***	0.573	0.446	**0.882****	**0.884****	0.645	0.249	0.036	-0.568
REEnonMag	0.096	0.097	0.372	-0.127	0.222	0.262	-0.019	0.380	**1.000****	0.674	-0.562

TABLE 4. Pearson Correlation (cont.)

SO_3	P_2O_5	K_2O	CaO	TiO_2	V_2O_5	Cr_2O_3	MnO	Fe_2O_3	CuO	ZnO	MoO_3	Eu_2O_3	Yb_2O_3	Re_20_7	LREE	HREE	TotalREE	REEmag	REEnonMag
1																			
-0.257	1																		
-0.730	**0.810***	1																	
0.341	-0.344	-0.525	1																
-0.651	-0.177	0.198	0.238	1															
-0.350	0.165	0.236	0.566	0.713	1														
-0.515	0.711	0.683	0.215	0.359	0.673	1													
-0.508	**0.933****	**0.939****	-0.519	-0.107	0.088	0.673	1												
-0.435	**0.810***	0.751	0.096	0.132	0.574	**0.944****	**0.792***	1											
-0.764*	**0.781***	**0.971****	-0.454	0.238	0.341	0.720	**0.915****	**0.793***	1										
-0.403	**0.918****	**0.894****	-0.574	-0.188	-0.063	0.576	**0.965****	0.686	**0.810***	1									
-0.257	-0.167	0.214	-0.300	-0.136	-0.251	-0.220	0.117	-0.031	0.171	0.127	1								
-0.631	**0.787***	**0.824***	-0.076	0.196	0.428	**0.933****	**0.840***	**0.934****	**0.856***	0.742	-0.039	1							
0.709	-0.167	-0.441	-0.330	-0.557	-0.612	-0.746	-0.311	-0.653	-0.52	-0.169	-0.167	-0.728	1						
-0.427	0.307	0.532	-0.740	-0.065	-0.524	0.013	0.480	-0.001	0.362	0.629	0.307	0.238	0.027	1					
-0.132	0.040	0.076	0.388	-0.171	0.087	0.383	0.152	0.443	0.123	0.080	0.404	0.448	-0.670	-0.088	1				
0.337	0.076	-0.231	**0.873***	0.214	0.687	0.464	-0.190	0.370	-0.197	-0.221	-0.485	0.142	-0.243	-0.647	0.185	1			
0.086	0.071	-0.070	**0.765***	-0.010	0.440	0.538	0.009	0.531	-0.016	-0.061	0.036	0.411	-0.631	-0.418	**0.844***	0.683	1		
-0.098	0.124	0.069	0.684	0.085	0.477	0.626	0.114	0.609	0.128	0.026	0.095	0.532	**-0.759***	-0.322	**0.883****	0.598	**0.982****	1	
0.921**	-0.231	-0.696	0.653	-0.466	-0.028	-0.243	-0.503	-0.198	-0.704	-0.439	-0.277	-0.446	0.404	-0.609	0.099	0.645	0.426	0.249	1

CONCLUSION

The Lenggoksono region had the highest concentration of SiO_2-dominant compounds in all samples. Neodymium (Nd) shows the most significant REE dominance, with total REE concentrations nearly three times that of the lowest element Terbium (Tb), indicating potential mineralization zones of interest for further exploration. The results of the interpolation mapping show that the element Ce has an even distribution throughout the Lenggoksono region and has the highest concentration at the LGSN 1 point. The magnetic susceptibility of igneous rocks (BBL 2) is lower than that of sand (WA 1). In the Pearson Correlation analysis, several REE elements are significantly correlated with oxide compounds and magnetic susceptibility, indicating the potential use of magnetic susceptibility as an effective and economical proxy in the exploration of critical minerals. The study's results suggest that certain critical minerals can be a marker of other critical minerals, and susceptibility can be used to indicate some critical minerals in natural materials.

ACKNOWLEDGMENTS

The authors are also grateful for the support of the SZ Geophysics research team. This research is supported by the Thesis Research Scheme of DRTPM with contract number 4.4.650/UN32.14.1/LT/2024.

REFERENCES

[1] D. B. Agusdinata, H. Eakin, and W. Liu, "Critical minerals for electric vehicles: A telecoupling review," *Environmental Research Letters*, vol. 17, no. 2, p. 013005, 2022, DOI: 10.1088/1748-9326/ac4763.

[2] I. D. Qurbani, R. J. Heffron, and A.T.S. Rifano, "Justice and critical mineral development in Indonesia and across ASEAN," *The Extractive Industries and Society*, vol. 8, no.1, pp. 355-362, 2021, DOI: 10.1016/j.exis.2020.11.017.

[3] B. A. Aziz, "Mineral Kritikal dari Perspektif Keselamatan Negara: Critical Minerals from a National Security Perspective," *International Journal of Interdisciplinary and Strategic Studies*, vol.2, no.3, pp. 145-156, 2021, DOI: 10.47548/ijistra.2021.38.

[4] A. Tonggiroh, "The Geochemical Character of Trace Elements in Coastal Sediments: Potential Implications of Metallic Mineral Resources on the West Coast of South Sulawesi, Indonesia," *Journal of Hunan University Natural Sciences*, vol/50, no.5, 2023, DOI: 10.55463/issn.1674-2974.50.5.8.

[5] N. A. Sasongko et al., "Trend of critical minerals utilization for Indonesia's Sustainable Energy Transition: A review," in *E3S Web of Conferences* vol. 513, p. 04004, EDP Sciences, 2024, DOI: 10.1051/e3sconf/202451304004.

[6] M. Arienzo et al., "Advances in the fate of rare earth elements, REE, in transitional environments: coasts and estuaries," *Water*, vol.14, no.3, p. 401, 2022, DOI: 10.3390/w14030401.

[7] I. A. R. Saputra, S. Aritonang, and M.D.M. Manessa, M. D. M., "Pemetaan Sumber Daya Rare Earth Elements (REE) Untuk Bahan Baku Industri Pertahanan dengan Metode Eksplorasi Geomarine," *Teknologi Penginderaan*, vol.1, no.1, 2019, DOI: 10.33172/tp.v1i1.483.

[8] C. Reimann et al., "GEMAS: Establishing geochemical background and threshold for 53 chemical elements in European agricultural soil," *Applied geochemistry*, 88, 302-318, 2018, DOI: 10.1016/j.apgeochem.2017.01.021.

[9] V. Balaram, "Advances in analytical techniques and applications in exploration, mining, extraction, and metallurgical studies of rare earth elements," *Minerals*, vol.13, no.8, p. 1031, 2023, DOI: 10.3390/min13081031.

[10] A. Susilo et al., "Inventory and identification of geodiversity to support geotourism in the Lenggoksono bay area of South Malang, Indonesia," in *Journal of Physics: Conference Series* vol. 1816, no. 1, p. 012111 IOP Publishing, 2021, DOI: 10.1088/1742-6596/1816/1/012111.

[11] S. John et al., "Earth Surface Processes, Landforms and Sediment Deposits: Rivers, alluvial plains, and fans," pp. 365-461, 2008, DOI: 10.1017/CBO9780511805516.014.

[12] S. Samsidar et al., "X-Ray Fluorescence Monitoring Metal Content and Nutrient Elements for Predicting Soil Fertility Parameters Based on pH in Ultisol Soil," *International Journal of Hydrological and Environmental for Sustainability*, vol.2, no.3, pp.104-112, 2023, DOI: 10.58524/ijhes.v2i3.290.

[13] M. Lucie, A. Francis, and Macdonald, "Petrography and Geochemistry of the Intrusive Rocks at the Diorite-Hosted Regnault Au Mineralization," *Minerals*, 12(2):128-128, 2022, DOI: 10.3390/min12020128.

[14] C. Maame et al., " Determination of trace elements and macronutrients in agricultural soils using energy dispersive X-ray fluorescence as a rapid and precise analytical technique," *The EGU General Assembly*, p.9564, 2020, DOI: 10.5194/EGUSPHERE-EGU2020-9564.

[15] V. Daniel et al., "Relating magnetic properties of municipal solid waste constituents to iron content – implications for enhanced landfill mining," vol.8, no.8, pp.31-46, 2019, DOI: 10.31025/2611-4135/2019.13876.

[16] N. Sharma et al., "Analysis of mineral elements in medicinal plant samples using LIBS and ICP-OES," *At. Spectrosc*, vol. 41, no.6, pp.234-241, 2020, DOI: 10.46770/AS.2020.06.003.

[17] S. R. Khan et al., "Inductively coupled plasma optical emission spectrometry (ICP-OES): a powerful analytical technique for elemental analysis," *Food Analytical Methods*, pp. 1-23, 2022, DOI: 10.1007/s12161-021-02148-4.

[18] C. Morrison et al., "Methods for the ICP-OES analysis of semiconductor materials," *Chemistry of Materials*, vol. 32, no. 5, pp.1760-1768, 2020, DOI: 10.1021/acs.chemmater.0c00255.

[19] Y. Han et al., "Fault monitoring using novel adaptive kernel principal component analysis integrating grey relational analysis," *Process Safety and Environmental Protection*, vol.157, pp.397-410, 2022, DOI: 10.1016/j.psep.2021.11.029.

[20] C. Liu et al., "Element case studies: rare earth elements," *Agromining: farming for metals: extracting unconventional resources using plants*, pp.471-483, 2021, DOI: 10.1007/978-3-030-58904-2_24.

[21] L. S. Xiao, "Scattered and Rare Earth Metals," in *Membrane-Based Separations in Metallurgy*, pp. 205-225 Elsevier, 2017, DOI: 10.1016/B978-0-12-803410-1.00007-4.

[22] K.R. Long et al., "The principal rare earth elements deposits of the United States: A summary of domestic deposits and a global perspective," *Springer* Netherlands, pp. 131-155, 2012, DOI: 10.1007/978-90-481-8679-2_7.

[23] P. L. Verplanckand M. W. Hitzman, "Rare earth and critical elements in ore deposits," *Society of Economic Geologists*, 2016, DOI: 10.5382/REV.18.

[24] J. A. Dearing, J. A. *Environmental magnetic susceptibility: using the Bartington MS2 system*. Chi Pub. 1994.

[25] Q. Liu et al., "Environmental magnetism: Principles and applications," *Reviews of Geophysics*, vol.50, no.4, 2012, DOI: 10.1029/2012RG000393.

[26] H. Pan et al., "Pearson correlation coefficient-based pheromone refactoring mechanism for multi-colony ant colony optimization," *Applied Intelligence*, vol.51, pp.752-774, 2021, DOI: 10.1007/s10489-020-01841-x.

[27] K. Okoye and S. Hosseini, "Correlation tests in R: pearson cor, kendall's tau, and spearman's rho," in *R Programming: Statistical Data Analysis in Research*, pp.247-277 Singapore: Springer Nature Singapore, 2024, DOI: 10.1007/978-981-97-3385-9_12.